CURRENT-DRIVEN DOMAIN WALL DYNAMICS AND ITS ELECTRIC SIGNATURE IN FERROMAGNETIC NANOWIRES

A Thesis

by

YANG LIU

Submitted to the Office of Graduate Studies of
Texas A&M University
in partial fulfillment of the requirements for the degree of

MASTER OF SCIENCE

August 2011

Major Subject: Physics

CURRENT-DRIVEN DOMAIN WALL DYNAMICS AND ITS ELECTRIC SIGNATURE IN FERROMAGNETIC NANOWIRES

A Thesis

by

YANG LIU

Submitted to the Office of Graduate Studies of
Texas A&M University
in partial fulfillment of the requirements for the degree of

MASTER OF SCIENCE

Approved by:

Co-Chairs of Committee,	Jairo Sinova
	Artem Abanov
Committee Members,	Tahir Cagin
	Igor Roshchin
Head of Department,	Edward Fry

August 2011

Major Subject: Physics

ABSTRACT

Current-driven Domain Wall Dynamics And Its Electric Signature In Ferromagnetic Nanowires. (August 2011)

Yang Liu, B.S, Beihang University

Co-Chairs of Advisory Committee: Dr. Jairo Sinova

Dr. Artem Abanov

We study current-induced domain wall dynamics in a thin ferromagnetic nanowire. We derive the effective equations of domain wall motion, which depend on the wire geometry and material parameters. We describe the procedure to determine these parameters by all-electric measurements of the time-dependent voltage induced by the domain wall motion. We provide an analytical expression for the time variation of this voltage. Furthermore, we show that the measurement of the proposed effects is within reach with current experimental techniques. We also show that a certain resonant time-dependent current moving a domain wall can significantly reduce the Joule heating in the wire, and thus it can lead to a novel proposal for the most energy efficient memory devices. We discuss how Gilbert damping, non-adiabatic spin transfer torque, and the presence of Dzyaloshinskii-Moriya interaction can effect this power optimization. Furthermore, we propose a new nanodot magnetic device. We derive a specific time-dependent current that is needed to switch the magnetization of the nanodot the most efficiently.

ACKNOWLEDGMENTS

I would like to thank my committee chairs, Dr. Abanov and Dr. Sinova, and my committee members, Dr. Roshchin and Dr. Cagin, for their guidance and support throughout the course of this research.

Thanks also go to my friends and colleagues, Dr. Tretiakov, Xiong-jun Liu and Xin Liu, and the department faculty and staff for making my time at Texas A & M University a great experience.

Finally, thanks to my mother and father for their encouragement.

TABLE OF CONTENTS

Page

ABSTRACT iii

ACKNOWLEDGMENTS iv

TABLE OF CONTENTS v

LIST OF FIGURES vi

1 INTRODUCTION 1

2 STATIC DOMAIN WALL IN FERROMAGNETIC NANOWIRES 4

3 THE EFFECTIVE EQUATIONS OF DOMAIN WALL MOTION 7

4 OHMIC LOSS MINIMIZATION BY RESONANT CURRENT* 9

5 MEASUREMENT OF THE PARAMETERS BY VOLTAGE 19

6 NANODOT MAGNETIC MEMORY DEVICE 28

7 SUMMARY 36

REFERENCES 37

VITA 38

LIST OF FIGURES

FIGURE Page

1.1 A sketch of racetrack memory 2

2.1 A moving head-to-head domain wall with the width Δ. 5

4.1 A schematic view of a current-driven domain wall in a ferromagnetic wire. 10

4.2 DW motion characteristics for dc currents. 12

4.3 Minimal power of Ohmic losses as a function of drift velocity 15

4.4 Resonant time-dependent current $J(\tau)$ with $\tau = Cj_c t$ for drift velocities $v_d = 0.5$ (dashed line) and $v_d = 4.5$ (solid line) for $a = 2$ (after Ref [9]). . 17

5.1 Dependence of average voltage $\langle V \rangle$ on dc current j for $C > 0$ and $C < 0$, respectively, see Eq. (5.3). 21

5.2 Fourier transform of the voltage V as a function of frequency f at dc current $1.1j_c$. 23

5.3 Input current j (dashed line) and measured voltage V (solid line) as functions of time t. 24

5.4 Voltage (solid line) evolution after the current (dashed line) is turned off at time t_i for $C > 0$ given by $\alpha = 0.02$ and $\beta = 0.01$. 26

6.1 A sketch of a current-driven domain wall in the concave ferromagnetic nanowire 28

6.2 Dependence of switching energy on switching time for $\sigma = 0.01$ (red doted line), $\sigma = 0.03$ (black dot-dashed line) and $\sigma = 0.05$ (green solid line). . . 34

6.3 Dependence of domain wall position and angle on time at optimal current. 35

1. INTRODUCTION

Recently, potential applications for the future memory and logic devices as well as important fundamental physics questions stimulated a number of experimental [1–4] and theoretical studies of the current-driven domain wall (DW) dynamics in ferromagnetic nanowires. It has been shown that DW can be moved by a current either parallel [1–3] or perpendicular to the wire. In some of these experiments short current pulses were employed to depin a DW from pinning sites [2, 3]. Furthermore, the topological electromotive force induced by DW dynamics in vortex DW has been studied both experimentally and theoretically.

In Section 3, we briefly review the method of collective coordinates [5] and apply it to find the dynamics of DW driven by both applied magnetic field and electric current. The effective equation of DW motion depend on the wire geometry and material parameters.

In Section 4, we study the optimization of the power supplied by electric current for the motion of domain walls in a nanowire. We show that a certain resonant time-dependent current moving a domain wall can significantly reduce the Joule heating in the wire, and thus it can lead to a novel proposal for the most energy efficient memory devices. We discuss how Gilbert damping [6], non-adiabatic spin transfer torque, and the presence of Dzyaloshinskii-Moriya interaction (DMI) [7, 8] can effect this power optimization.

In Section 5 , we study a simultaneous all-electric manipulation of DWs and measurement of their dynamics. We describe three independent procedures to determine parameters of the DW dynamics [9] directly by measuring the time-dependent voltage caused by the DW motion. The magnitude of the proposed effects is within current

This thesis follows the style of Physical Review Letters.

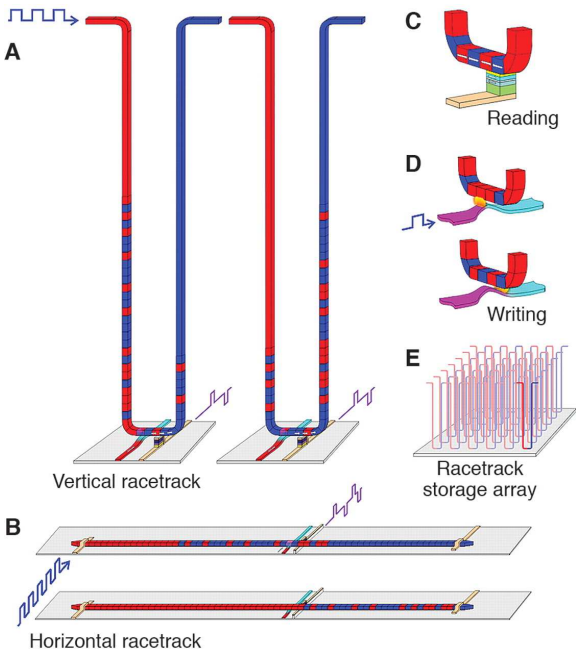

Fig. 1.1. A sketch of racetrack memory. The racetrack is a ferromagnetic nanowire, with data encoded as a pattern of magnetic domains along a portion of the wire (after [10]).

experimental resolution. For the magnetic field driven DWs, similar techniques have already shown promise.

In Section 6, we also present the domain wall dynamics in concave nanowires. The proposed magnetic domain wall racetrack memory devices [10] (as shown in Fig. 1.1) require the speed of DW to be of the order of spin wave velocity in order to compete with existing charge memory devices. We propose a nano dot device, which employs the magnetization direction within the domain wall as the information storage. Without current, the domain wall stays at the place where the wire cross section is the narrowest; and we derive a specific time-dependent current that is needed to switch the nano dot.

2. STATIC DOMAIN WALL IN FERROMAGNETIC NANOWIRES

Ferromagnetic materials, such as iron, cobalt and permalloy, could exhibit spontaneous magnetization in the absence of external magnetic field below its Curie temperature because of the exchange interaction between the localised magnetic moments. Above the Curie temperature, local magnetic moments are disordered, thus the material can no longer maintain a spontaneous magnetization. In this thesis, we only consider ferromagnetic materials with a high Curie temperature such as permalloy (with Curie temperature up to 853 K). For such materials, thermal fluctuation of the magnetization can be neglected in the room temperature.

The magnetization in such case can be described by a classical continuous unit magnetization vector-$\mathbf{S}(z) = \mathbf{M}/M$, where $\mathbf{M}$ is the magnetization vector. Then the exchange interaction energy density has the form:

$$J(\nabla \mathbf{S})^2.$$

Here J is the exchange interaction constant. This interaction prohibits large gradients of $\mathbf{S}$ since the energy is minimized when the ferromagnetic moments are along the same direction.

In real materials, there are the crystalline anisotropy and the shape anisotropy. The origin of the crystalline anisotropy is microscopic, while the origin of the shape anisotropy is the dipole-dipole interaction. The shape anisotropy we discussed in this thesis is always inversion invariant. In this thesis, we consider ferromagnetic nanowires with typical size 100×10 nm^2. The width of the wire is much smaller then any characteristic length of the magnetic structure, but is large enough so that the total spin in a cross section is large. Therefore, we still can treat the unit magnetization vector $\mathbf{S}(z)$ as a classical continuous vector field which depends only on one coordinate. The wire is along the z-axis, as shown in Fig. 2.1. The shape

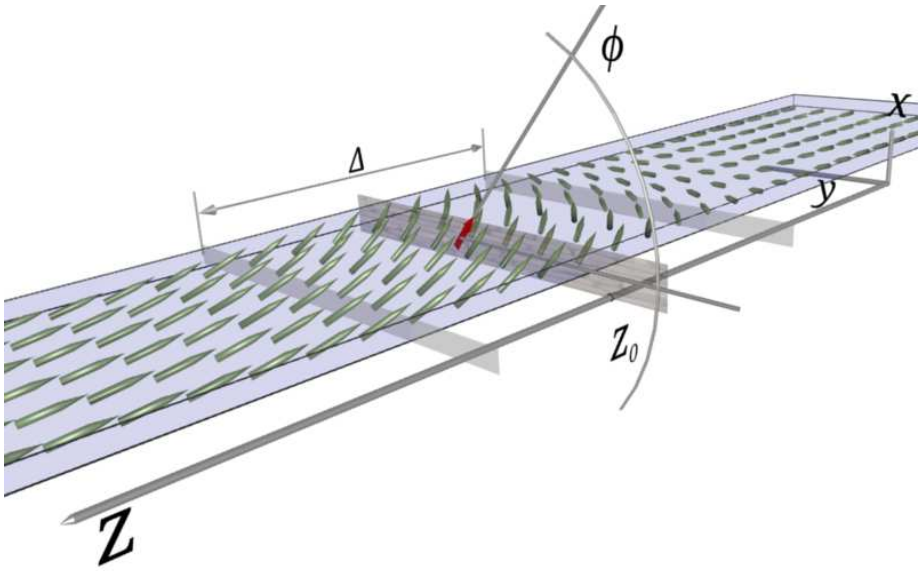

Fig. 2.1. A moving head-to-head domain wall with the width Δ. DW is centered at z_0 and is tilted by angle ϕ.

anisotropy in the wire has a strong uniaxial component (anisotropy constant λ) and a weak component in the transverse plane (anisotropy constant K).

The shape anisotropy along the wire has energy density:

$$-\lambda S_z^2.$$

It is lowest when the magnet moments are aligned with z direction thus increases the domain wall width. The time reversal-invariant Hamiltonian has two distinct ground states: all spins along $+z$ or all spins along $-z$ direction. A DW is a crossover from one ground state to another. The DW could be either head-to-head or tail-to-tail. Such a configuration is a result of a balance between exchange and anisotropy energies. Its width ($\Delta \propto \sqrt{\frac{J}{\lambda}}$) are typically around 50 nm for such wires.

In a wire, there are two collective coordinates to describe the dynamics of DW: the position of DW (z_0) and the direction of the spin the center of DW (ϕ). If the wire is translationally invariant, the DW energy does not depend on z_0. All the other terms in the energy density are much smaller and only slightly change the shape of DW.

In this thesis, we neglect the pinning of the DW by impurities and wire imperfections.

3. THE EFFECTIVE EQUATIONS OF DOMAIN WALL MOTION

The dynamics of magnetization $\mathbf{S}$ in a quasi-one-dimensional wire is described by Landau-Lifshitz-Gilbert (LLG) equation with the current j [6–8, 11, 12],

$$\dot{\mathbf{S}} = -\mathbf{S} \times \mathbf{H}_e - j\partial_z \mathbf{S} + \beta j \mathbf{S} \times \partial_z \mathbf{S} + \alpha \mathbf{S} \times \dot{\mathbf{S}}, \tag{3.1}$$

where $\mathbf{H}_e = -\delta\mathcal{H}/\delta\mathbf{S}$ is the effective magnetic field given by the Hamiltonian $\mathcal{H}$ of the system, $\mathbf{S} = \mathbf{M}/|M|$ is a unit magnetization vector, the wire is along z direction, α is Gilbert damping constant, β is non-adiabatic spin torque constant, $\partial_z \equiv \partial/\partial z$, and the time is measured in the units of the gyromagnetic ratio $\gamma_0 = g|e|/(2mc)$; and the current j is measured in units of $a^3/(2eM\gamma_0)$ where a is the lattice constant.

We consider a solution of the static one-dimensional LLG equation (3.1) without a current,

$$\mathbf{S}_0(z) \times \mathbf{H}_e(z) = 0, \quad \mathbf{H}_e(z) = \delta\mathcal{H}/\delta\mathbf{S}_0(z), \tag{3.2}$$

which has zero modes. It means that there exists a two-dimensional vector $\boldsymbol{\xi}$ such that $\mathbf{S}_0(z, \boldsymbol{\xi})$ is a solution of $\mathbf{S}_0 \times \mathbf{H}_e = 0$ for any $\boldsymbol{\xi}$ in some continuous two-dimensional interval.

Assuming now that there is a small correction $\mathbf{h}$ to the static LLG equation $\mathbf{S}_0 \times \mathbf{H}_e = 0$, we expect a time dependent solution of the LLG equation

$$\dot{\mathbf{S}} = \mathbf{S} \times \frac{\delta\mathcal{H}}{\delta\mathbf{S}} + \mathbf{h} \tag{3.3}$$

The correction $\mathbf{h}$ comes from three terms: the first is from the correction to the Hamiltonian itself, the second is from dissipation and current, and the third is from external magnetic field.

$$\mathbf{h} = \mathbf{S}_0 \times \frac{\delta\mathcal{H}_\delta}{\delta\mathbf{S}_0} + \mathbf{h}_j - \vec{S}_0 \times \vec{H}, \tag{3.4}$$

where $\mathcal{H}_\delta$ is the correction to the Hamiltonian.

$$\mathbf{h}_j = -j\partial_z \mathbf{S} + \beta j \mathbf{S} \times \partial_z \mathbf{S} + \alpha \mathbf{S} \times \dot{\mathbf{S}} \tag{3.5}$$

Using the expression in the supplemental material in [5]:

$$\begin{aligned} \dot{\xi}_i \frac{1}{2} \int dz\, \epsilon^{kk'} \mathbf{S}_0(z) \times \partial_{\xi_k} \mathbf{S}_0(z) \cdot \partial_{\xi_{k'}} \mathbf{S}_0(z) \\ = -\epsilon^{ij} \int dz\, \mathbf{S}_0(z) \times \partial_{\xi_j} \mathbf{S}_0(z) \cdot \mathbf{h}(z)\,, \end{aligned} \tag{3.6}$$

where ϵ^{ij} is the Levi-Civita symbol, and identifying $\xi_1 \equiv z_0$, and $\xi_2 \equiv \phi$ in Eq. (3.6). The general equation of DW motion has form:

$$\dot{z}_0 = Aj + B(j - j_c \sin(2\phi)) - E\frac{\partial_{z_0} E_\delta}{2} - FH, \tag{3.7}$$

$$\dot{\phi} = C(j - j_c \sin(2\phi)) + D\frac{\partial_{z_0} E_\delta}{2} + GH \tag{3.8}$$

Here

$$A = \frac{\tilde{\beta}}{\tilde{\alpha}}, \quad B = \frac{\tilde{\alpha} - \tilde{\beta}}{\tilde{\alpha}}(1 + \tilde{\alpha} a_{z\phi}), \quad C = (\tilde{\alpha} - \tilde{\beta}) a_{zz}, \quad j_c = \frac{\tilde{\alpha}}{\tilde{\alpha} - \tilde{\beta}}\kappa, \tag{3.9}$$

$$F = \frac{\alpha a_{\phi\phi}}{1 + \alpha^2(a_{zz}a_{\phi\phi} - a_{z\phi}^2)}, \qquad G = \frac{1 - \alpha a_{z\phi}}{1 + \alpha^2(a_{zz}a_{\phi\phi} - a_{z\phi}^2)}, \tag{3.10}$$

$$D = \frac{\gamma_0}{A_0 M} G, \qquad E = \frac{\gamma_0}{A_0 M} F, \tag{3.11}$$

$$\tag{3.12}$$

where $\tilde{\alpha} = \alpha\mathcal{D}$, $\tilde{\beta} = \beta\mathcal{D}$, $\mathcal{D} = \sqrt{a_{zz}a_{\phi\phi} - a_{z\phi}^2}$, $a_{zz} = \frac{1}{2}\int dz (\partial_z \mathbf{S}_0)^2$, $a_{\phi\phi} = \frac{1}{2}\int dz (\partial_\phi \mathbf{S}_0)^2$, and $a_{z\phi} = \frac{1}{2}\int dz \partial_z \mathbf{S}_0 \cdot \partial_\phi \mathbf{S}_0$.

Eqs. (3.9) and (3.9) are consistent [1] with the expressions for A, B, C, and j_c found in Ref. [5].

[1] For the Hamiltonian used in Ref. [5], $\mathcal{D} = 1$, $a_{z\phi} = \Gamma\Delta$, $a_{zz} = (1 + \Gamma^2\Delta^2)/\Delta$, and $\Gamma = D/J$, where D and J are, respectively, the Dzyaloshinskii-Moriya and exchange interaction constants.

4. OHMIC LOSS MINIMIZATION BY RESONANT CURRENT*

Due to its direct relevance to future memory and logic devices, the dynamics of domain walls (DW) in magnetic nanowires has become recently a very popular topic. [10, 13, 14] There are mainly two goals which scientists try to achieve in this field. One goal is to move the domain walls with higher velocity in order to make faster memory or computer logic. The other one is inspired by the modern trend of energy conservation and concerns a power optimization of the domain-wall devices.

Generally, the domain walls can be manipulated whether by a magnetic field [14, 15] or electric current [1, 10]. Although the latter method is preferred for industrial applications due to the difficulty with the application of magnetic fields locally to small wires. For this reason, we consider in this thesis the current induced domain-wall dynamics. We make a proposal on how to optimize the power for the DW motion by means of reducing the losses on Joule heating in ferromagnetic nanowires. [9] Moreover, because the averaged over time (often called drift) velocity of a DW generally increases with applied current, we also address the first goal. Namely, we can move the DWs with higher current densities without burning the wire by the excessive heat and thus archive higher drift velocities of DWs. The central idea of this proposal is to employ resonant time-dependent current to move DWs, where the period of the current pulses is related to the periodic motion of DW internal degrees of freedom.

The schematic view of a domain wall in a narrow ferromagnetic wire is shown in Fig. 4.1. These DWs are characterized by their width Δ which is mainly determined by exchange interaction and anisotropy along the wire λ. Another important quantity is the transverse anisotropy across the wire K, which governs the pinning of the

*Reprinted with permission from "Minimization of Ohmic Losses for Domain Wall Motion in a Ferromagnetic Nanowire" by O. A. Tretiakov, Y. Liu, and Ar. Abanov, 2010. Phys. Rev. Lett. **105**, 217203 (2010). Copyright(2010) by The American Physical Society.

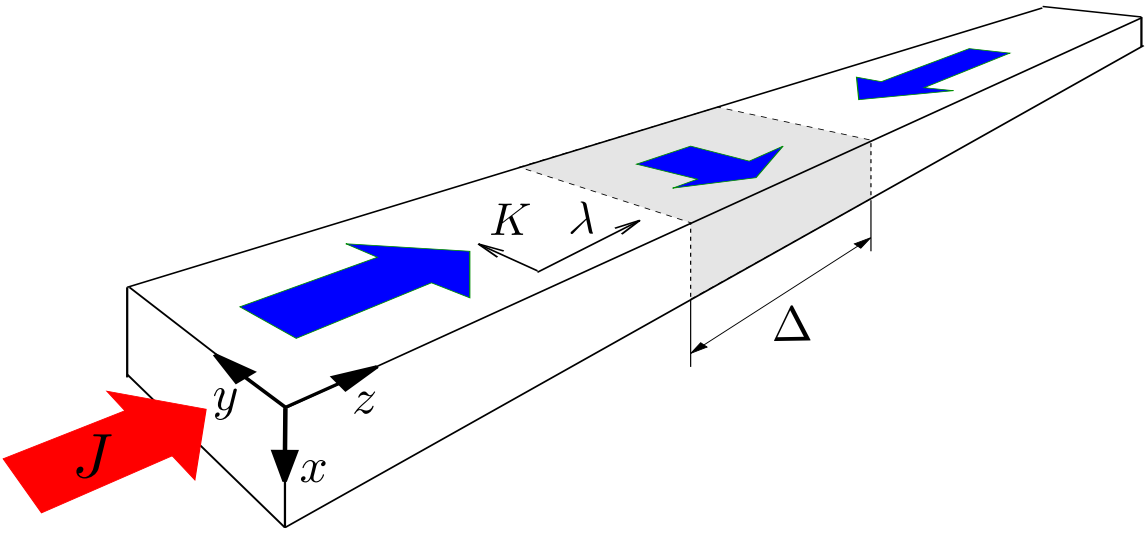

Fig. 4.1. A schematic view of a current-driven domain wall in a ferromagnetic wire. The DW width is Δ (after Ref [9]).

transverse component of the DW magnetization. When no current is applied to the wire, it leads to two degenerate positions of the transverse magnetization component of the wall, as shown in Fig. 4.1. One position is along y direction, the other is along $-y$ direction.

In this section, we only consider DW driven by current in a translationally invariant nanowire. Thus, the equations of DW motion have form:

$$\dot{z}_0 = AJ + B[J - j_c \sin(2\phi)], \tag{4.1}$$

$$\dot{\phi} = C[J - j_c \sin(2\phi)], \tag{4.2}$$

where $J(t)$ is a time-dependent current. The coefficients A, B, C, and critical current j_c can be evaluated for a particular model in terms of α, β and other microscopic parameters. Following Ref. [5], for the model with Dzyaloshinskii-Moriya interaction one can find $A = \beta/\alpha$, $B = (\alpha-\beta)(1+\alpha\Gamma\Delta)/[\alpha(1+\alpha^2)]$, $C = (\alpha-\beta)\Delta/[(1+\alpha^2)\Delta_0^2]$, and $j_c = (\alpha K\Delta/|\alpha-\beta|)[\pi\Gamma\Delta/\sinh(\pi\Gamma\Delta)]$, where $J_{\rm ex}$ is exchange constant, D is DMI constant, and $\Gamma = D/J_{\rm ex}$. Also, $\Delta = \Delta_0/\sqrt{1-\Gamma^2\Delta_0^2}$, where Δ_0 is the DW width in the absence of DMI.

Alternatively, Eqs. (4.1) and (4.2) can be obtained in a more general framework by means of symmetry arguments. We note that because of the translational invariance $\dot{z}_0$ and $\dot{\phi}$ cannot depend on z_0. Furthermore, to the first order in small transverse anisotropy K, $\dot{\phi}$ and $\dot{z}_0$ are proportional to the first harmonic $\sin(2\phi)$. Then, the expansion in small current J up to a linear in J order gives Eqs. (4.1) and (4.2). In this case the coefficients A, B, C, and j_c have to be determined directly from experimental measurements [4].

For the dc current applied to the wire, the DW dynamics governed by Eqs. (4.1) and (4.2) can be obtained explicitly [5]. For $J < j_c$ and $A \neq 0$ the DW only moves along the wire and is tilted on angle ϕ_0 from the transverse-anisotropy easy axis given by condition $\sin(2\phi_0) = J/j_c$. The drift velocity is $V_d = \langle \dot{z}_0(J) \rangle = AJ$, see Eq. (4.1).

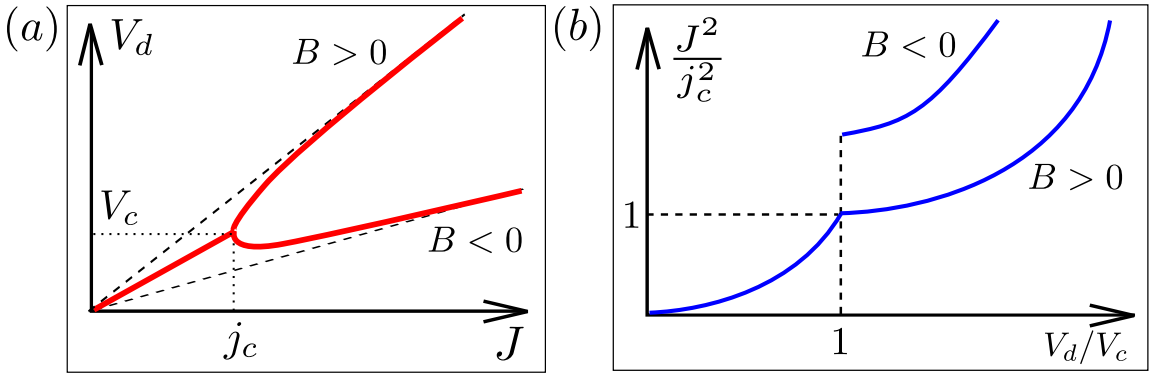

Fig. 4.2. DW motion characteristics for dc currents. (a) Drift velocity V_d of DW as a function of current J for $B > 0$ and $B < 0$, see Eq. (4.1). The slope at $J < j_c$ is given by A, whereas at $J \gg j_c$ it is $A+B$. (b) Power of Ohmic losses $p_{\rm dc}(V_d/V_c) = J^2/j_c^2$ as a function of drift velocity V_d. For $B < 0$ the power has a discontinuity at $V_d/V_c = 1$ (after Ref [9]).

Therefore, the linear slope of $V_d(J)$ below j_c gives constant A, as shown in Fig. 4.2. The value of j_c is determined as the endpoint of this linear regime. At $J = j_c$, the magnetization angle becomes perpendicular to the easy axis, $\phi_0 = \pi/2$. For $J > j_c$, the DW both moves and rotates, and Eqs. (4.1) and (4.2) give $V_d = AJ + B\sqrt{J^2 - j_c^2}$, so that the slope of $V_d(J)$ at large J gives $A + B$.

The largest losses in the nanowire with a DW are the Ohmic losses of the current. In general, the influence of the DW on the resistance is negligible and therefore we can assume that the resistance of the wire is constant with time. Then the time-averaged power of Ohmic losses is proportional to $\langle J^2(t)\rangle$. Since the resistance is almost constant, in this thesis we will calculate $P = \langle J^2(t)\rangle$ and loosely call it the power of Ohmic losses. Our goal is to minimize the Ohmic losses while keeping the DW moving with a given constant drift velocity.

For the following it will be convenient to introduce the dimensionless variables for time, drift velocity, current, power, and the ratio of slopes of $V_d(J)$ at large and small currents,

$$\tau = C j_c t, \quad v_d = \frac{V_d}{V_c}, \quad j = \frac{J}{j_c}, \quad p = \frac{\mathcal{P}}{j_c^2}, \quad a = \frac{A+B}{A}. \tag{4.3}$$

Although we note that in the special case of $\alpha = \beta$, it can be shown that $C = B = 0$ and one cannot use dimensionless variables (4.3). However, in this case the DW dynamics is trivial [16]: the DW does not rotate $\phi = 0, \pi$ and moves with the velocity $\dot{z}_0 = J$.

First, we consider the case of dc current and the power as a function of drift velocity. For $v_d < 1$ we find $p_{\rm dc} = v_d^2$. For currents above j_c the power $p_{\rm dc}(v_d) = j^2$ is given in terms of drift velocity $v_d = j + (B/A)\sqrt{j^2 - 1}$ as shown in Fig. 4.2 (b). The power is quadratic in v_d, and for $B < 0$ it has a discontinuity at $v_d = 1$.

In general, the DW motion has some period T and current $j(\tau)$ must be a periodic function with the same T to minimize the Ohmic losses. Measuring the angle from

the hard axis instead of easy axis and scaling it by 2, i.e, $2\phi = \theta - \pi/2$, we can write the dimensionless current drift velocity as [9]

$$j(\tau) = \dot{\theta}/2 - \cos\theta, \quad v_d = \frac{a}{2}\langle\dot{\theta}\rangle - \langle\cos\theta\rangle, \tag{4.4}$$

where $\dot{\theta} = \partial\theta/\partial\tau$.

To minimize the power of Ohmic losses, we need to find the minimum of $\langle j^2(\tau)\rangle$ at fixed v_d,

$$\overline{p} = \left\langle (\dot{\theta}/2 - \cos\theta)^2 - 2\rho(a\dot{\theta}/2 - \cos\theta - v_d) \right\rangle, \tag{4.5}$$

where we use a Lagrange multiplier 2ρ to account for the constraint given by v_d from Eq. (4.4). Power (4.5) can be considered as an effective action for a particle in a periodic potential U, and its minimization gives the equation of motion $\ddot{\theta}/2 = -\partial U/\partial\theta$ which in turn can be reduced to

$$\dot{\theta} = \pm 2\sqrt{d - U(\theta,\rho)}, \quad U(\theta,\rho) = -\cos^2\theta - 2\rho\cos\theta. \tag{4.6}$$

where d is an arbitrary constant. Since changing $\rho \to -\rho$ in U of Eq. (4.6) is equivalent to changing $\theta \to \pi + \theta$, below we can consider only positive ρ.

Eq. (4.6) shows that there are two different regimes: (1) the bounded regime where $d < \max[\mathrm{U}(\theta,\rho)]$ in which case θ is bounded, and the particle oscillates in potential well $U(\theta)$, see inset of Fig. 4.3 (a); and (2) the rotational regime where $d > \max[\mathrm{U}(\theta,\rho)]$ with freely rotating magnetization in the DW.

In the bounded regime, the particle moves between the two turning points $-\theta_0$ and θ_0 given by $d = U(\pm\theta_0,\rho)$. Since θ is a bounded function $\langle\dot{\theta}\rangle = 0$ and $v_d = -\langle\cos\theta\rangle$. One can show [9] that in this regime, the power of Ohmic losses is minimal for dc current, i.e., $\overline{p} = v_d^2$.

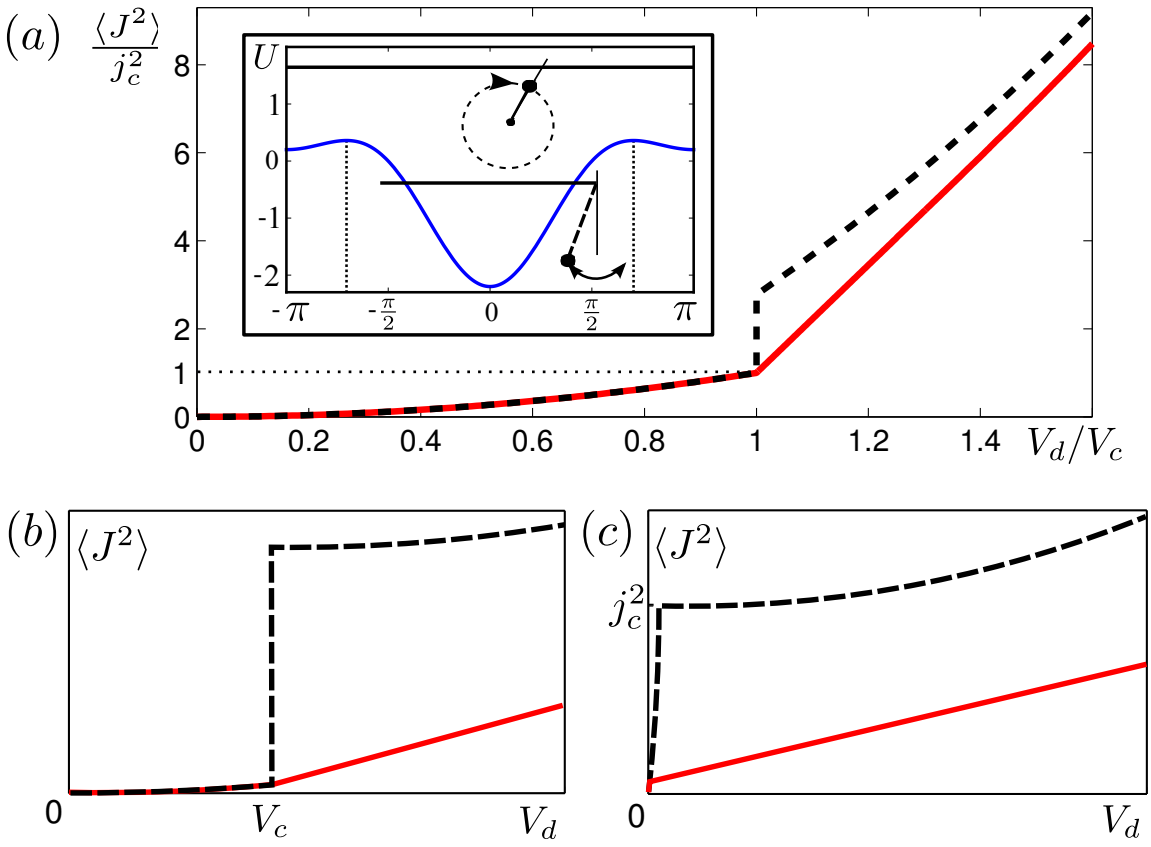

Fig. 4.3. Minimal power of Ohmic losses as a function of drift velocity. (a) Minimal power of Ohmic losses $\overline{p} = \langle J^2\rangle/j_c^2$ as a function of drift velocity V_d shown by solid line for $a = 0.5$. The dashed line depicts $\overline{p}$ for dc current. The inset shows the potential $U(\theta)$ in which a "particle" is moving in the bounded (pendulum-like) and unbounded (rotational) regimes. A sketch of $\langle J^2\rangle(V_d)$ shown by solid line in (b) for $\beta \gg \alpha$ ($a \ll 1$) and (c) for $\beta \ll \alpha$ ($a \gg 1$)(after Ref [9]).

In the rotational regime, the term in Eq. (4.4) with $\langle\dot{\theta}\rangle$ should be kept because θ is not bounded. The equation of motion is the same as for a nonlinear oscillator. [9] Using the minimization condition $\partial\overline{p}/\partial\rho|_{v_d} = 0$, one finds

$$\int_{-\pi}^{\pi}\sqrt{d - U(\theta,\rho)}d\theta = 2\pi a\rho. \tag{4.7}$$

This equation defines the relationship between d and ρ.

The results for the minimal power of Ohmic losses $\overline{p}(v_d)$ are presented in Fig. 4.3. For $a > 1$ there is a critical velocity $v_{\rm rc} < 1$, such that at $v_d < v_{\rm rc}$ the power of Ohmic losses is $\overline{p} = v_d^2 = p_{\rm dc}$. Above $v_{\rm rc}$ one can minimize the Ohmic losses by moving DW with resonant current pulses. Right above $v_{\rm rc}$ there is a certain range of v_d where $\overline{p} = 2\rho_0 v_d - \rho_0^2$ with $\rho_0(a) < 1$ given by Eq. (4.7) with $d = \rho^2$. The critical velocity is found as $v_{\rm rc} = \rho_0(a)$. For $a < 1$, see e.g. Fig. 4.3 (a), we find that $v_{\rm rc} = 1$, whereas at $v_d > 1$ minimal power $\overline{p}$ is significantly lower than $p_{\rm dc}$. Immediately above $v_d = 1$, we find that there is a range of v_d where $\overline{p}$ is linear in v_d. At large v_d the minimal power is always smaller than $p_{\rm dc}$, the difference between them then approaches $p_{\rm dc} - \overline{p} = (1 - 1/a)^2/2$.

We note that even in the limiting cases of the systems with weak ($\beta \ll \alpha$) or strong ($\beta \gg \alpha$) non-adiabatic spin transfer torque, see Fig. 4.3 (b) and (c), where the power of Ohmic losses is high for dc currents, the optimized ac current gives dramatic reduction in heating power thus greatly expanding the range of materials which can be used for spintronic devices. [10, 14] We also note that DMI suppresses critical current j_c and affects parameter a.

For $v_d < v_{\rm rc}$, the optimal current coincides with the dc current, above $v_{\rm rc}$ the resonant current $j(t)$ is plotted in Fig. 4.4 for $a = 2$ and two different velocities v_d. At $v_d > v_{\rm rc}$, the current's maximum $j_{\rm max}$ increases from $2 - v_{\rm rc}$ at small enough $v_d < 1$ up to $j_{\rm max} \approx v_d/a$ at $v_d \gg 1$. The current's minimum increases monotonically from small positive values $j_{\rm min} = v_{\rm rc}$ at $v_d \sim 1$ up to $j_{\rm min} = j_{\rm max} - 2|1 - a|/a$ at $v_d \gg 1$. At $v_d < 1$ (for $a > 1$), the time between the current picks decreases with increasing velocity as $T \simeq (\pi a - 2 \arcsin v_{\rm rc})/(v_d - v_{\rm rc})$, whereas the pick's width is given by $\approx 1.3/\sqrt{(1 - v_{\rm rc})}$. Therefore, at small $v_d - v_{\rm rc}$ the picks are widely separated, then as v_d increases the time between the picks decreases. At $v_d \gg 1$ the optimal current has a large constant component and small-amplitude ac modulations on top of it.

We have studied the current driven DW dynamics in thin ferromagnetic wires. The ultimate lower bound for the Ohmic losses in the wire has been found for any

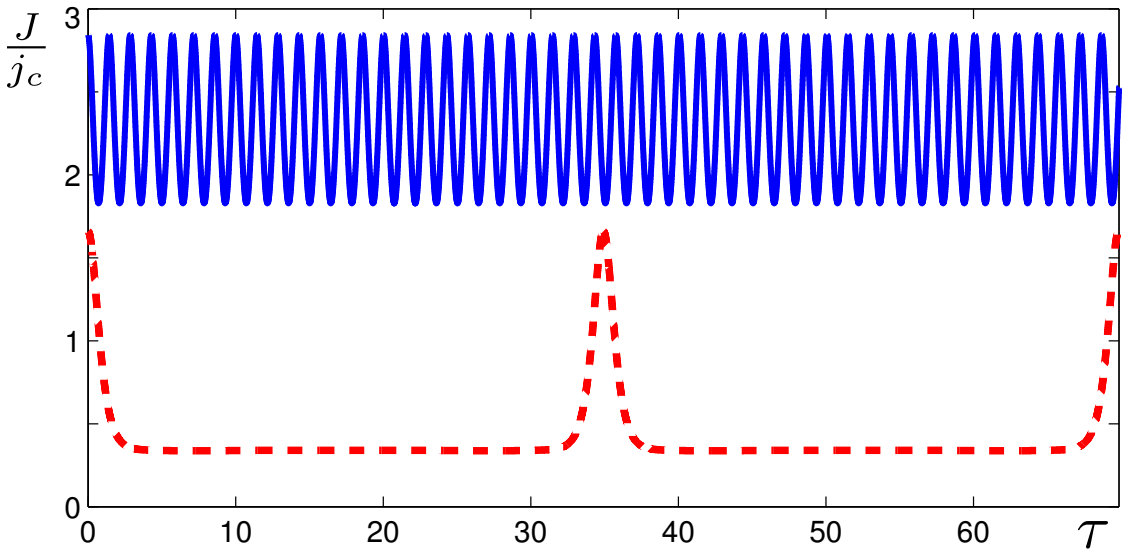

Fig. 4.4. Resonant time-dependent current $J(\tau)$ with $\tau = Cj_c t$ for drift velocities $v_d = 0.5$ (dashed line) and $v_d = 4.5$ (solid line) for $a = 2$ (after Ref [9]).

DW drift velocity V_d. We have obtained the explicit time-dependence of the current which minimizes the Ohmic losses. We believe that the use of these resonant current pulses instead of dc current can help to dramatically reduce heating of the wire for any V_d.

5. MEASUREMENT OF THE PARAMETERS BY VOLTAGE

Microscopically, the dynamics parameters have been found in Section 2. Now, we outline the method to find A, B, C, and j_c in Section 4 directly from all-electric experimental measurements. This method is based on measurements of voltage V induced by a moving DW. To find the ac voltage V one has to know the time evolution of the total energy (per unit area of the wire's cross-section) in the system,

$$\dot{E} = \int dz \frac{\delta \mathcal{H}}{\delta \mathbf{S}} \cdot \dot{\mathbf{S}}(z). \tag{5.1}$$

In general, DW energy has two contributions: the power supplied by electric current and negative contribution due to dissipation in the wire. Using the general solution of LLG equation (3.1), one can obtain the derivative of energy as

$$\dot{E} = 2[\beta a_{zz}\dot{z}_0 + (1-\beta a_{z\phi})\dot{\phi}]j - \alpha \int dz \dot{\mathbf{S}}_0^{\,2}. \tag{5.2}$$

Here, the last term on the right-hand side of Eq. (5.2) describes the dissipation and therefore is always nonpositive. Meanwhile, the first term is proportional to current density j and gives the power Vj supplied by current. With the help of Eqs. (3.9) and adopting approximation $\mathcal{D} \simeq 1$ of Ref. [5], we obtain the expression for the induced DW voltage [1],

$$V = \frac{A^2 C}{B} j + C(1+A)[j - j_c \sin(2\phi)]. \tag{5.3}$$

Note that Eq. (5.3) gives the contribution to voltage due to DW motion. This contribution is additional to the usual Ohmic one. The voltage V in Eq. 5.3 is measured in units of $Pg\mu_B/(e\gamma_0)$ and the current density is measured in units $2eM/(Pg\mu_B)$,

[1] Since in majority of materials both $\alpha \ll 1$ and $a_{z\phi} = \Gamma\Delta \ll 1$, we can be safely neglect $\alpha\Gamma\Delta$ compared to 1 in Eq. 5.3.

where P is the current polarization. We emphasize that unlike in the earlier studied cases this voltage is not caused by the motion of topological defects (vortices) transverse to the wire.

In order to find coefficients A, B and C, we propose three independent measurements of voltage induced by moving DW. Although there are various factors affecting the nanowire resistance, the contributions from most of them are independent of DW motion and therefore give only a constant component of the resistance. To characterize the DW dynamics, one has to concentrate only on the resistance variations in time. Our estimates show that the amplitude of voltage oscillations due to DW motion is of the order of 10^{-7} V and therefore is experimentally measurable.

Eq. (5.3) implies that the voltage of DW can give all the necessary information about DW dynamics. Namely, one can obtain coefficient C by measuring the voltage changing with time and coefficients A and B by measuring the amplitude of the voltage oscillations.

In Refs. [9], it was proposed to obtain A, B, and j_c by measuring the drift velocity of DW. It is important to note that Eq. (5.3) has the same form as Eq. (4.1). Thus, instead of measuring the drift velocity, which requires a more complicated experimental setup, we propose to perform all-electric measurements. Namely, to measure the average voltage of DW, $\langle V \rangle$, as a function of dc current. From Eq. (5.3), one can see that $\langle V \rangle = \frac{A^2 C}{B} j$ for $j < j_c$, whereas $\langle V \rangle = \frac{A^2 C}{B} j + (1+A) C \sqrt{j^2 - j_c^2}$ for $j > j_c$, as shown in Fig. 5.1. The critical current is determined by the end of the linear in j region at small currents. The measurement of slope k_1 at $j < j_c$, and slope k_2 at $j \gg j_c$ gives the two independent quantities:

$$k_1 = \frac{A^2 C}{B}, \tag{5.4}$$

$$k_2 - k_1 = (1+A)C. \tag{5.5}$$

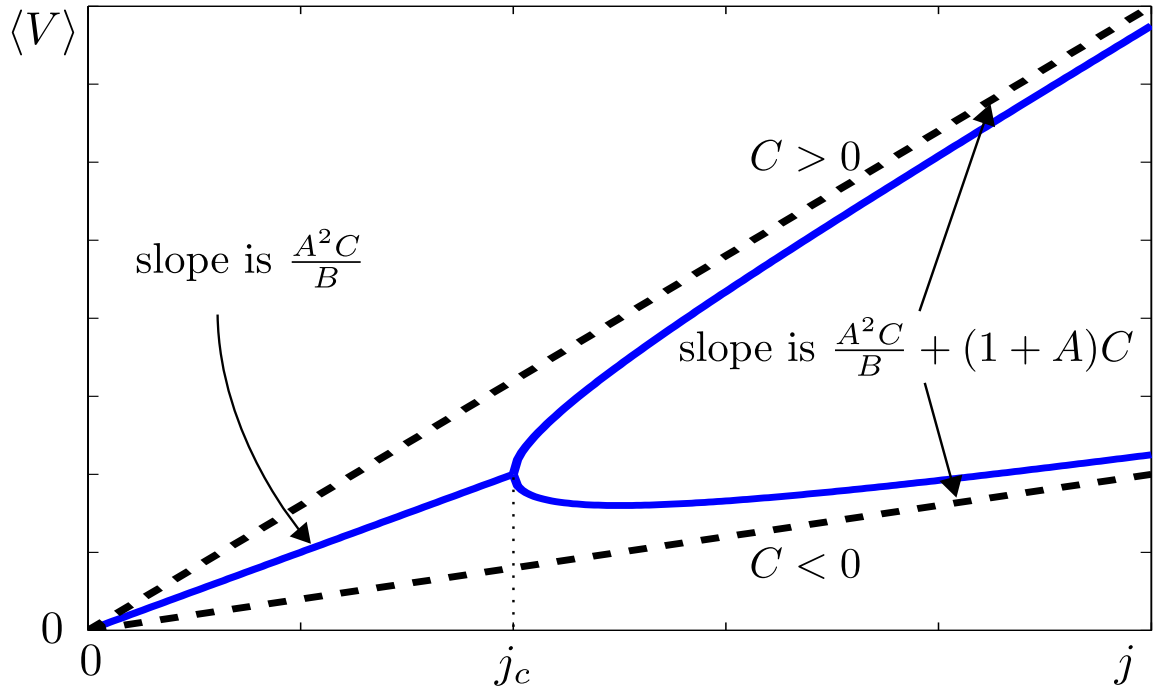

Fig. 5.1. Dependence of average voltage $\langle V \rangle$ on dc current j for $C > 0$ and $C < 0$, respectively, see Eq. (5.3). The slope at $j < j_c$ gives $\frac{A^2 C}{B}$, whereas at $j \gg j_c$ it gives $\frac{A^2 C}{B} + (1 + A)C$.

Alternatively, instead of measuring voltage average for dc current, one can input a linearly increasing with time current $j(t) = qt$ below the critical value j_c. At sufficiently small q, the voltage will also be linear in time, $V(t) \approx \frac{A^2C}{B}qt$. By measuring this voltage one can find

$$\frac{V(t)}{j(t)} = \frac{A^2C}{B}. \tag{5.6}$$

Once C is determined, Eqs. (5.4) and (5.5) give A and B. The drawback of this measurement is that it might be hard to disentangle k_1 and k_2 from the Ohmic contribution experimentally. However, $k_2 - k_1$ is free from the Ohmic resistance of the wire.

In order to find C, the most intuitive idea is to input a dc current slightly above j_c. Then the voltage induced by moving DW will oscillate with the period of double angle ϕ, see the insets to Fig. 5.2. The half-width of the peak (dip) for $C > 0$ ($C < 0$) is given by $\arccos(j_c/j)/(|C|\sqrt{j^2 - j_c^2})$. The measurement of the period T_0 of the voltage oscillations (which we estimate to be $\sim 10^{-7} \sim 10^{-6}$ s) determines at a given j coefficient C as follows:

$$|C| = \frac{1}{T_0}\int_0^{\pi} \frac{d\phi}{j - j_c \sin(2\phi)} = \frac{\pi}{T_0\sqrt{j^2 - j_c^2}}. \tag{5.7}$$

For $j - j_c \ll j_c$, the period diverges but the half-width $\sim 1/(Cj_c)$ stays finite. To obtain period T_0, one can perform the Fourier transform of $V(t)$ to find frequency $f_0 = 1/T_0$, as shown in Fig. 5.2.

To determine coefficient A in the same experiment, one can measure $\Delta V = V_{max} - V_{min} = 2(1 + A)|C|j_c$, see insets of Fig. 5.2. Then

$$A = \frac{\Delta V}{2|C|j_c} - 1. \tag{5.8}$$

Note that $\Delta V = 2(k_2 - k_1)j_c$ and therefore this experiment can also provide a crosscheck with the aforementioned slopes measurement.

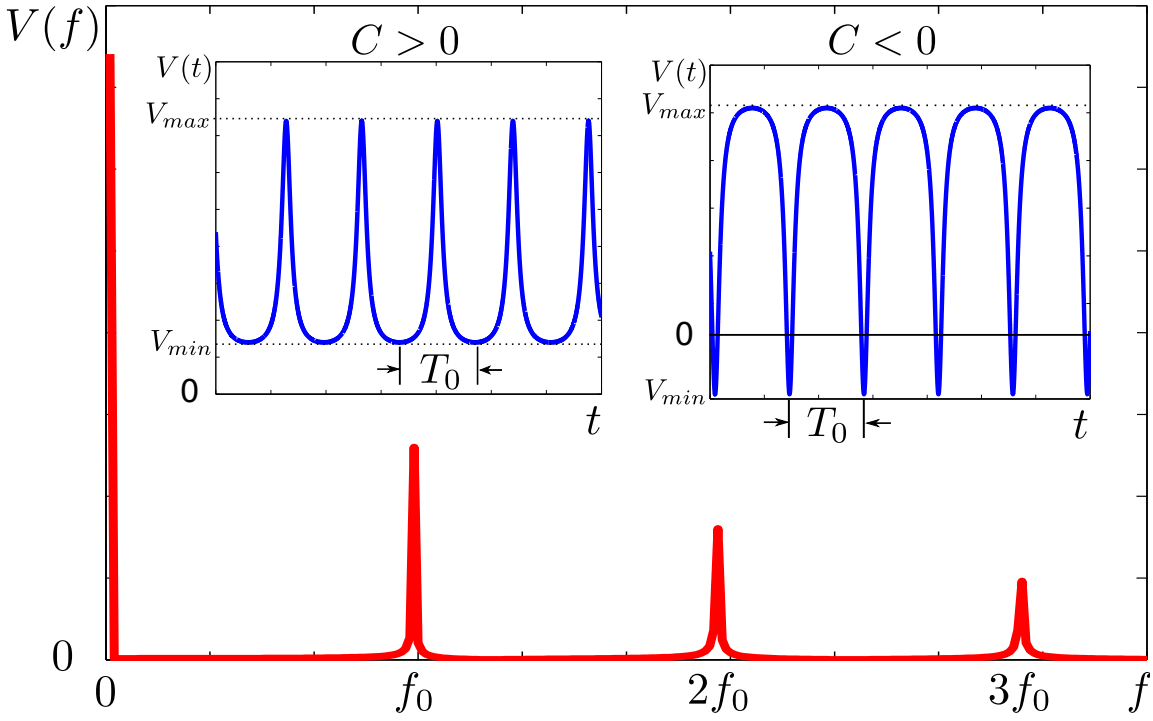

Fig. 5.2. Fourier transform of the voltage V as a function of frequency f at dc current $1.1j_c$. The insets show V as a function of time t for $C > 0$ given by $\alpha = 0.02$ and $\beta = 0.01$; and for $C < 0$ given by $\alpha = 0.01$ and $\beta = 0.02$. The voltage period is $T_0 = 1/f_0$. In the inset for $C < 0$, the voltage varies between $V_{max} = 0.041j_c/\Delta$ and $V_{min} = -0.019j_c/\Delta$.

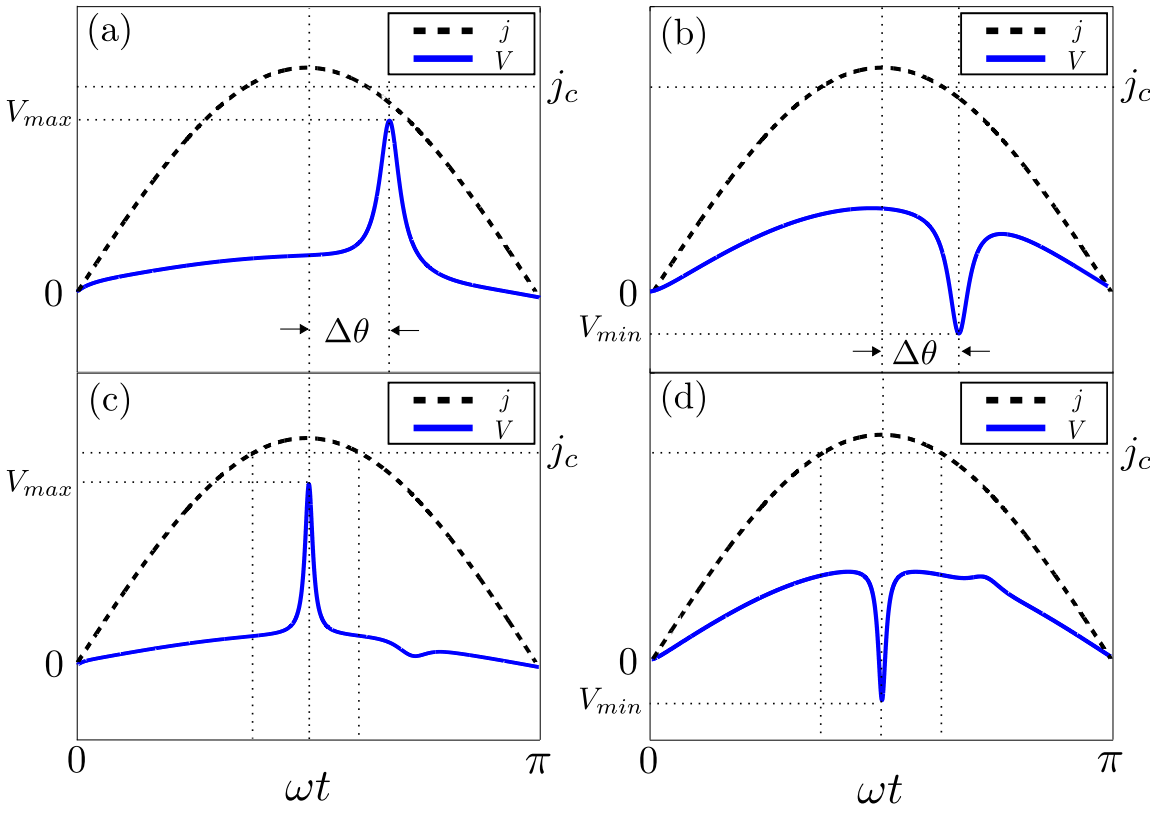

Fig. 5.3. Input current j (dashed line) and measured voltage V (solid line) as functions of time t. (a) and (b) show the phase delay $\Delta\theta$ between the current maximum and voltage extremum for $C > 0$ and $C < 0$, respectively. (c) and (d) depict $V(t)$ at $\Delta\theta = 0$ for the same $C > 0$ and $C < 0$, respectively.

Another method to measure the coefficient C is by inputting ac current $j = j_0 \sin \omega t$ with $j_0 > j_c$, which has only a short time interval where $j > j_c$, so that there is only one period of voltage within the period of $j(t)$. One can measure the phase delay, $\Delta\theta$, between the current maximum and voltage extremum [2], as can be seen in Fig. 5.3. Next, one fixes the amplitude j_0 and tunes the frequency ω until $\Delta\theta = 0$. In this case, for $j_0 - j_c \ll j_c$, we can use a half of the time interval for which the current pulse is above j_c to approximate the period of ϕ by dc current j_0 as

$$\frac{1}{2\omega}\left(\pi - 2\arcsin\frac{j_c}{j_0}\right) \approx \frac{\pi}{|C|\sqrt{j_0^2 - j_c^2}}. \tag{5.9}$$

For $j_0 - j_c \ll j_c$, Eq. (5.9) can be further simplified to give

$$|C| \approx \frac{\pi\omega}{2(j_0 - j_c)}. \tag{5.10}$$

In other words, when $\omega \approx C(j_0 - j_c)$ which corresponds roughly to $\omega \sim 10^7$ Hz, the current pulse covers only one period of voltage. Our simulations show that the approximate expression (5.10) works sufficiently well for $j_0 \leq 1.3 j_c$. The sign of C is determined by the extremum of the measured voltage: $C > 0$ if V has the minimum and $C < 0$ if V has the maximum.

In addition to the large peak (dip) of voltage (Fig. 5.3) there is a smaller one with the opposite curvature. That is because when $j(t)$ reaches j_c, the angle ϕ has not rotated yet to the angle corresponding to $\sin(2\phi_0) = 1$ due to the cumulative phase delay between current and voltage.

It is also possible to measure the coefficient C for currents below the critical value j_c. The constant $|C|j_c$ determines the internal time scale of the DW motion. After one switches the subcritical current off at time t_i, the voltage asymptotically decays as $\exp(-2|C|j_c t)$, see Fig. 5.4. One can measure the decay of $V(t)$ with time.

[2] Our simulations show that the initial phase of angle ϕ does not affect the phase delay, since the time it takes for the current to increase from 0 to j_c is long enough to adjust the initial angle to the one corresponding to $\sin(2\phi) \approx j/j_c$.

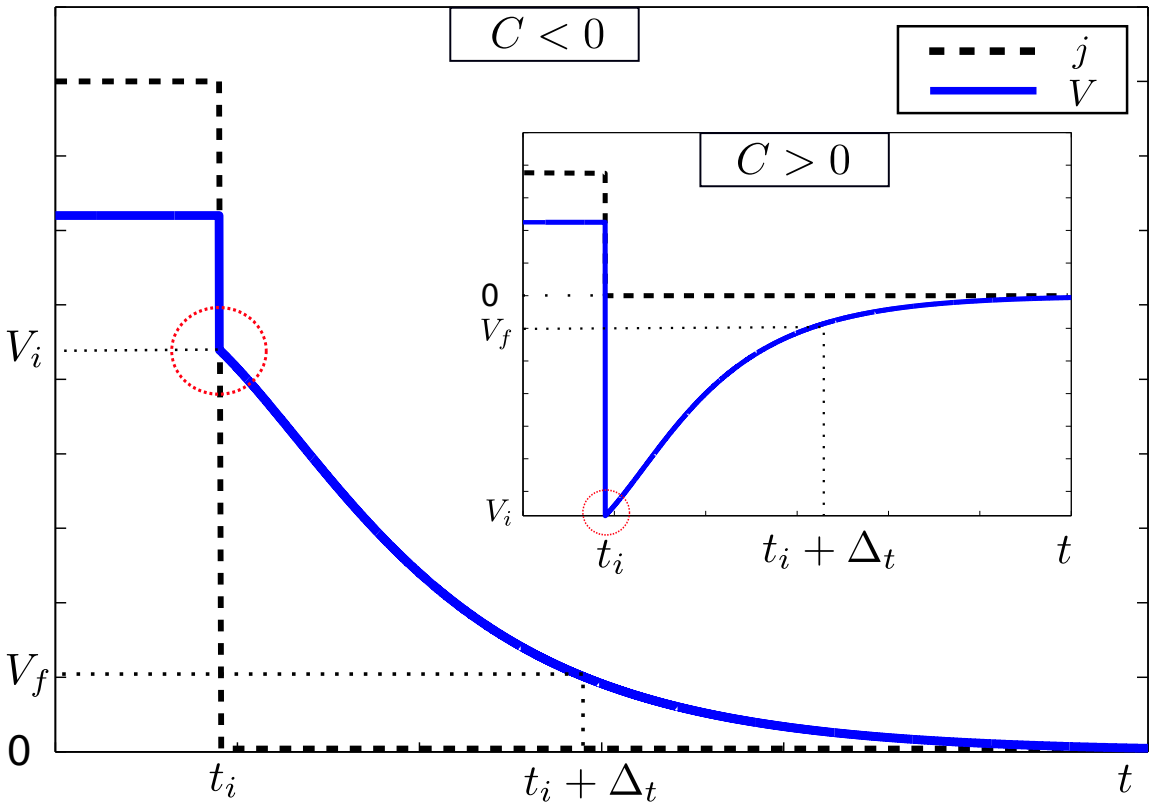

Fig. 5.4. Voltage (solid line) evolution after the current (dashed line) is turned off at time t_i for $C > 0$ given by $\alpha = 0.02$ and $\beta = 0.01$. Inset: the same dependencies for $C < 0$ given by $\alpha = 0.01$ and $\beta = 0.02$. The measurement of V_f is performed at $t_i + \Delta_t$. The region sketched by the dotted circle cannot be described within our approach but it is too small to effect our results.

It can be done in the following way: one inputs a dc current below j_c, and then measures voltage V_i immediately after turning off the current at t_i, and then later measures voltage V_f at time $t_i + \Delta_t$. We note that right after turning off the current, there is a short time period when the DW dynamics cannot be described by our equations. It corresponds to the dynamics of fast degrees of freedom. This process has a characteristic time $\sim 10^{-11}s$ which is typically much smaller than the voltage decay time $\sim 10^{-8}$ s. We thus can safely assume that the rotation angle ϕ does not change much during this time interval, and we find

$$|C| \simeq \frac{1}{2\Delta_t j_c} \ln \frac{2V_i/V_f}{1+\sqrt{1-j^2/j_c^2}}, \tag{5.11}$$

which is valid for $V_i/V_f \gg 1$. For example, estimating $V_i/V_f = 10$ we find $|C| \approx 1.17/(\Delta_t j_c)$. The sign of C can be easily determined by the form of voltage decay, see Fig. 5.4.

6. NANODOT MAGNETIC MEMORY DEVICE

In this section, we propose a nanodot magnetic device, as shown in Fig. 6.1. First, we show the domain wall dynamics in concave nanowires with the general equations of DW motion found in Section 3. In this case, the Hamiltonian has a correction due to the shape change of the nanowire.

$$\dot{z}_0 = Aj + B(j - j_c \sin(2\phi)) - E\frac{\partial_{z_0}\xi_\delta}{2}, \tag{6.1}$$

$$\dot{\phi} = C(j - j_c \sin(2\phi)) + D\frac{\partial_{z_0}\xi_\delta}{2}, \tag{6.2}$$

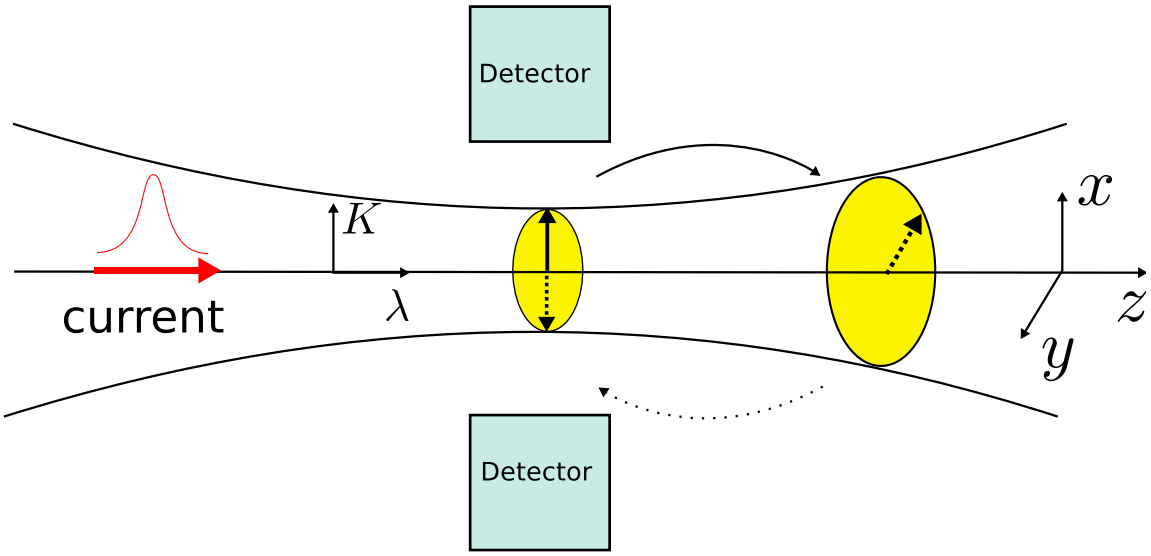

Fig. 6.1. A sketch of a current-driven domain wall in the concave ferromagnetic nanowire. An appropriate spin polarized pulse drives DW to rotate and move along z direction. In the end, the DW moves back to the original position with opposite magnetization direction.

where A, B, C and j_c are the same definition in [9]. We can approximate the parameters:

$$D = \frac{\gamma_0}{A_0 M}\frac{1-\alpha a_{z\phi}}{1+\alpha^2(a_{zz}a_{\phi\phi}-a_{z\phi}^2)} \approx \frac{\gamma_0}{A_0 M}\frac{1}{1+\alpha^2}, \tag{6.3}$$

$$E = \frac{\gamma_0}{A_0 M}\frac{\alpha a_{\phi\phi}}{1+\alpha^2(a_{zz}a_{\phi\phi}-a_{z\phi}^2)} \approx \Delta D. \tag{6.4}$$

Eq. (6.1)- Eq. (6.2) imply that if the energy is minimum at the original position, domain wall moves back when the current is turned off. Thus, we can flip the magnetization direction at the same position with an appropriate current pulse.

It is instructive to introduce the dimensionless equation of motion. First, let's write B, C in a much simpler fashion considering $\alpha \ll 1$, $\Gamma\Delta \ll 1$.

$$B = \frac{(\alpha-\beta)(1+\alpha\Gamma\Delta)}{\alpha(1+\alpha^2)} \approx \frac{\alpha-\beta}{\alpha}, \tag{6.5}$$

$$C = \frac{(\alpha-\beta)(1+\Gamma^2\Delta^2)}{\Delta} \approx \frac{\alpha-\beta}{\Delta}, \tag{6.6}$$

$$\kappa \doteq \frac{\alpha-\beta}{\alpha}. \tag{6.7}$$

We introduce the dimensionless quantities:

$$z_0 \to z_0/\Delta, \quad t \to t/\frac{\Delta}{\kappa j_c}, \quad j \to j/\kappa j_c, \quad 2\varphi \to \theta \tag{6.8}$$

and rewrite Eq.(6.1-6.2) as

$$\dot{z}_0 = j - \sin\theta - \eta z_0, \tag{6.9}$$

$$\frac{1}{2}\dot{\theta} = (\alpha-\beta)\dot{z}_0 - \beta\sin\theta + \sigma z_0, \tag{6.10}$$

where

$$\sigma = \frac{\Delta}{\kappa j_c}\frac{\gamma_0}{A_0 M}\frac{\partial_{z_0} E_\delta}{2} = \frac{J\Delta}{\kappa j_c}\frac{\gamma_0}{M A_0}\frac{h_0}{R}, \tag{6.11}$$

$$\eta = \alpha\sigma. \tag{6.12}$$

Now let's suppose a nanowire with symmetric concave shape, for example, the wire width $w(z)$ is a concave function symmetric function, which has a minimum at $z = 0$. Then the energy of domain wall is given by

$$\mathcal{H} = \frac{J}{2\Delta^2}\int dz\{1 - S_z^2\}A(z) \tag{6.13}$$

$$\approx \frac{J}{\Delta}A(z_0), \tag{6.14}$$

since $1 - S_z$ is non-zero only around z_0. We can expand the wire width to the second order,

$$w(z_0) = w(0) + z_0 w'(0) + \frac{z_0^2}{2}w''(0) + \cdots \tag{6.15}$$

Since it's concave, $w'(0) = 0$, $w''(0) = 1/R$, where R is the curvature radius around $z = 0$. Then, the cross section of the wire is given by

$$A(z_0) = h_0 w(z_0) \approx w_0 h_0 + \frac{h_0}{R}\frac{z_0^2}{2}, \tag{6.16}$$

where h_0 is the constant strip thickness. The correction to the domain wall energy due to the shape change is given by

$$E_\delta = 2\frac{h_0}{R}\frac{J}{\Delta}\frac{z_0^2}{2} = \frac{z_0^2}{R w_0}E_0. \tag{6.17}$$

We can estimate σ with gyromagnetic ratio $\gamma_0 = 1.76 \times 10^{11}$ rad $\cdot$ s^{-1} $\cdot$ T^{-1}; T = V $\cdot$ s/m^2; exchange constant $J = 1.3 \times 10^{-11}$ J/m; magnetization $M = 8 \times 10^5$ A/m; $j_c = 100$ m/s.

$$\sigma \approx \frac{\Delta}{w_0 R} \times 10 \text{ nm} \tag{6.18}$$

For example, when $R = 300$ nm, $\Delta = 30$ nm, $\sigma \approx 0.01$. Notice that $\alpha \ll 1$, thus $\eta \ll 1$ we can safely neglect ηz_0 term in Eq.(6.10) in all consideration below.

With the help of Eqs. (6.9)-(6.10), we get

$$\frac{1}{2\sigma}\ddot{\theta} + \frac{\alpha}{\sigma}\dot{\theta}\cos\theta + \sin\theta = j + \frac{\alpha - \beta}{\sigma}\dot{j}. \tag{6.19}$$

The motion of θ mimics pendulum motion with dumping and external force. Without current, the system oscillates with infinite time in theory.

In this part, we minimize the Ohmic losses while following the boundary conditions

$$\theta(0) = 0, \quad z_0(0) = 0, \tag{6.20}$$

$$\theta(T) = 2\pi, \quad z_0(T) = 0, \tag{6.21}$$

where T is the switching time.

In order to minimize the Ohmic losses, we need to find the minimum of $\int_0^T j^2 dt$ at fixed constraint given by Eq.(6.10),

$$\mathcal{L} = \int_0^T [(\dot{z}_0 + \sin\theta)^2 - \lambda((\alpha - \beta)\dot{z}_0 - \frac{1}{2}\dot{\theta} - \beta\sin\theta + \sigma z_0)]dt. \tag{6.22}$$

Here, to account for the constraint given by Eq.(6.10), we use a Lagrange multiplier λ. With respect to three functions $z_0(t)$, $\theta(t)$, and $\lambda(t)$, we get the following set of equations:

$$\ddot{z}_0 + \dot{\theta}\cos\theta + \frac{\sigma}{2}\lambda - \frac{\alpha-\beta}{2}\dot{\lambda} = 0 \tag{6.23}$$

$$(\dot{z}_0 + \sin\theta)\cos\theta - \frac{1}{4}\dot{\lambda} + \frac{\beta}{2}\lambda\cos\theta = 0 \tag{6.24}$$

$$-\frac{1}{2}\dot{\theta} + \sigma z_0 + (\alpha-\beta)\dot{z}_0 - \beta\sin\theta = 0 \tag{6.25}$$

Let us introduce a function $J(t)$ such that

$$J(0) = 0, \quad \dot{J}(t) = -\lambda(t). \tag{6.26}$$

Then the Eq. (6.23)- Eq. (6.25) become

$$\dot{z}_0 + \sin\theta - \frac{\sigma}{2}J + \frac{\alpha-\beta}{2}\dot{J} = j_0, \tag{6.27}$$

$$(\dot{z}_0 + \sin\theta)\cos\theta + \frac{1}{4}\ddot{J} - \frac{\beta}{2}\dot{J}\cos\theta = 0, \tag{6.28}$$

$$-\frac{1}{2}\dot{\theta} + \sigma\dot{z}_0 + (\alpha-\beta)\dot{z}_0 - \beta\sin\theta = 0. \tag{6.29}$$

Now, we can use shooting method to solve this boundary value problem by tuning j_0 and $\dot{J}(0)$.

Let us consider $\alpha = \beta = 0$ case for simplicity. The equation of motion becomes,

$$\dot{z}_0 + \sin\theta - \frac{\sigma}{2}J = j_0, \tag{6.30}$$

$$(\dot{z}_0 + \sin\theta)\cos\theta + \frac{1}{4}\ddot{J} = 0, \tag{6.31}$$

$$z_0 = \frac{1}{2\sigma}\dot{\theta}, \tag{6.32}$$

and finally

$$\frac{1}{2\sigma}\partial_t^2\left(\frac{1}{2\sigma}\ddot{\theta} + \sin\theta\right) + \left(\frac{1}{2\sigma}\ddot{\theta} + \sin\theta\right)\cos\theta = 0 \tag{6.33}$$

Since $\sigma \ll 1$, so if characteristic time of the experiment T is such that $T \ll 1/\sqrt{\sigma}$ then all the terms except the fourth derivative can be dropped and we get

$$\partial_t^4 \theta = 0 \tag{6.34}$$

In fact, for a more general case, the correction to the domain wall energy is arbitrary concave symmetric function $f(z)$. This solution still holds, but the current depends on the specific form of $f(z)$.

Using the boundary conditons for θ and z_0, we find

$$\theta(t) = 6\pi(t/T)^2 - 4\pi(t/T)^3, \tag{6.35}$$

which gives

$$j(t) = \frac{1}{2\sigma}\ddot{\theta} + \sin\theta \approx \frac{6\pi}{\sigma T^2}(1 - 2t/T). \tag{6.36}$$

And the flipping energy, as shown in Fig. 6.2, is given by

$$\int_0^T j(t)^2 dt = \frac{12\pi^2}{\sigma^2 T^3}. \tag{6.37}$$

Comparing the analytic solution (Eq. (6.36)) with our simulation, as can be seen in Fig. 6.3, we find that our linear current coincides with the simulation result for short flipping time, i.e. $T < 1/\sqrt{\sigma}$. For long flipping time, the optimal current just flip the domain wall and then let it oscillate around $z = 0$ and $\theta = 2\pi$ until the required time.

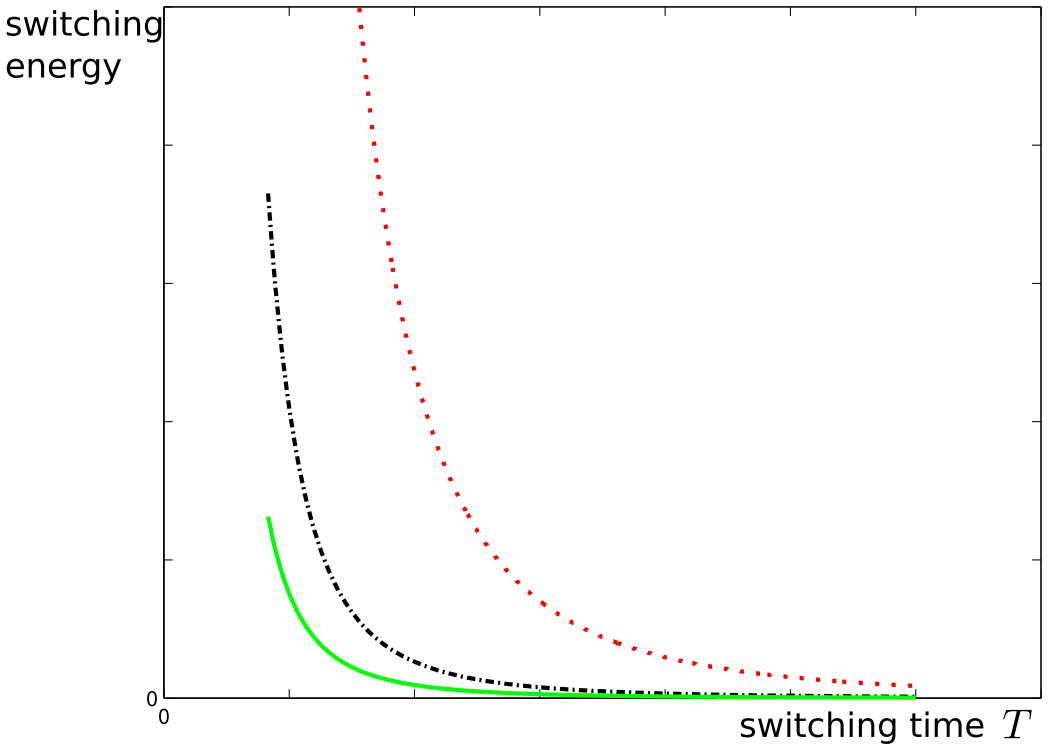

Fig. 6.2. Dependence of switching energy on switching time for $\sigma = 0.01$ (red doted line), $\sigma = 0.03$ (black dot-dashed line) and $\sigma = 0.05$ (green solid line).

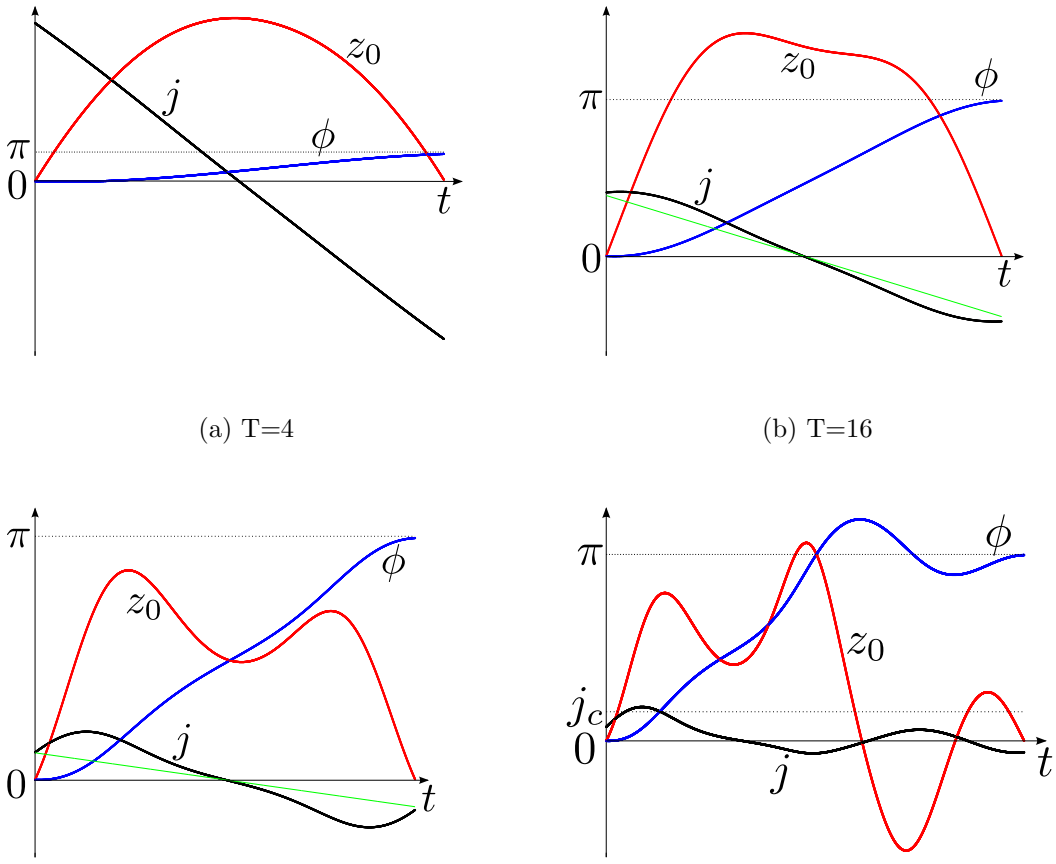

(a) T=4 (b) T=16

(c) T=30 (d) T=55

Fig. 6.3. Dependence of domain wall position and angle on time at optimal current. Optimal current $j(t)$ (black line), analytic solution of optimal current (green line), z_0 (red line) and θ (blue line) as a function of time for different switching times T for $\alpha = 0.01$, $\beta = 0.02$, $\sigma = 0.03$.

7. SUMMARY

In Section 3, we reviewed the method of collective coordinates [5] and applied it to find the dynamics of DW driven by both applied magnetic field and electric current. The effective equation of DW motion depend on the wire geometry and material parameters. In Section 4, we studied the optimization of the power supplied by electric current for the motion of domain walls in a nanowire. We showed that a certain resonant time-dependent current moving a domain wall could significantly reduce the Joule heating in the wire, and thus it could lead to a novel proposal for the most energy efficient memory devices. We discussed how Gilbert damping, non-adiabatic spin transfer torque, and the presence of Dzyaloshinskii-Moriya interaction can effect this power optimization. In Section 5, we studied a simultaneous all-electric manipulation of DWs and measurement of their dynamics. We described three independent procedures to determine parameters of the DW dynamics [9] directly by measuring the time-dependent voltage caused by the DW motion. The magnitude of the proposed effects is within current experimental resolution. In Section 6, we proposed a nanodot magnetic memory device and a specific time-dependent current that is needed to switch the nanodot most efficiently. The result in Ohmic losses minimization allows us to move the DWs with higher current densities without burning the wire by excessive heat, thus, build faster memory devices. The proposed nanodot device gives promise of a nonvolatile memory device.

REFERENCES

[1] A. Yamaguchi, T. Ono, S. Nasu, K. Miyake, K. Mibu, and T. Shinjo, Phys. Rev. Lett. **92**, 077205 (2004).

[2] L. Thomas, M. Hayashi, X. Jiang, R. Moriya, C. Rettner, and S. S. P. Parkin, Nature **443**, 197 (2006).

[3] L. Thomas, M. Hayashi, X. Jiang, R. Moriya, C. Rettner, and S. Parkin, Science **315**, 1553 (2007).

[4] S. A. Yang, G. S. D. Beach, C. Knutson, D. Xiao, Q. Niu, M. Tsoi, and J. L. Erskine, Phys. Rev. Lett. **102**, 067201 (2009).

[5] O. A. Tretiakov and Ar. Abanov, Phys. Rev. Lett. **105**, 157201 (2010).

[6] T. L. Gilbert, Phys. Rev. **100**, 1243 (1955).

[7] I. Dzyaloshinsky, J. Phys. Chem. Solids **4**, 241 (1958).

[8] T. Moriya, Phys. Rev. **120**, 91 (1960).

[9] O. A. Tretiakov, Y. Liu, and Ar. Abanov, Phys. Rev. Lett. **105**, 217203 (2010).

[10] S. S. P. Parkin, M. Hayashi, and L. Thomas, Science **320**, 190 (2008).

[11] Z. Li and S. Zhang, Phys. Rev. Lett. **92**, 207203 (2004).

[12] A. Thiaville, Y. Nakatani, J. Miltat, and Y. Suzuki, Europhys. Lett. **69**, 990 (2005).

[13] D. A. Allwood, G. Xiong, M. D. Cooke, C. C. Faulkner, D. Atkinson, N. Vernier, and R. P. Cowburn, Science **296**, 2003 (2002).

[14] D. A. Allwood, G. Xiong, C. C. Faulkner, D. Atkinson, D. Petit, and R. P. Cowburn, Science **309**, 1688 (2005).

[15] T. Ono, H. Miyajima, K. Shigeto, K. Mibu, N. Hosoito, and T. Shinjo, Science **284**, 468 (1999).

[16] S. E. Barnes and S. Maekawa, Phys. Rev. Lett. **95**, 107204 (2005).

VITA

Yang Liu received his Bachelor of Science degree in physics from Beihang University in 2008 and Master of Science in physics from Texas A&M University in 2011.

Mr. Yang Liu can be reached at Department of Physics, Texas A&M University, 4242 TAMU, College Station, TX 77843-4242. His email address is walkingroland@gmail.com.